Coherent Optical Detection of Highly Excited Rydberg States Using Electromagnetically Induced Transparency

A. K. Mohapatra, T. R. Jackson, and C. S. Adams

Department of Physics, Durham University, Rochester Building, South Road, Durham DH1 3LE, United Kingdom

(Received 22 December 2006; published 15 March 2007)

We demonstrate coherent optical detection of highly excited Rydberg states (up to $n = 124$) using electromagnetically induced transparency (EIT), providing a direct nondestructive probe of Rydberg energy levels. We show that the EIT spectra allow direct optical detection of electric field transients in the gas phase, and we extend measurements of the fine structure splitting of the nd series up to $n = 96$. Coherent coupling of Rydberg states via EIT could also be used for cross-phase modulation and photon entanglement.

DOI: 10.1103/PhysRevLett.98.113003 PACS numbers: 32.80.Rm, 03.67.Lx, 34.60.+z, 42.50.Gy

Rydberg atoms display rich many-body behavior [1–6] and make attractive candidates for fast quantum gates [7,8] due to their enhanced two-body interactions. In addition, the strong dipole-dipole coupling could be exploited to realize a photonic phase gate using electromagnetically induced transparency (EIT) involving a Rydberg state [9]. Rydberg atoms are produced by direct laser excitation or coherently using stimulated Raman adiabatic passage [10,11] and are detected indirectly via the ions or electrons produced by an ionization pulse [1]. This detection technique provides high efficiency but is destructive, and the atom cannot be reused. For quantum information applications, a nondestructive detection of the Rydberg state is preferable. One possibility is EIT [12], which is manifest as an absence of absorption or an associated rapid variation in the dispersion allowing dissipation-free sensing of the desired atomic resonance. EIT has been widely studied in atomic vapors [13], frequently using a Λ scheme where a coherence is induced between two ground states. Alternatively, in the ladder scheme the coherence is induced between a ground state and an excited state via an intermediate state [14]. Previously, excited d states with a principal quantum number up to $n = 8$ have been observed via optical probing of a ladder system [15].

In this work, we present experimental results on an EIT ladder system involving highly excited Rydberg states with $n = 26$–124. We show that the nondestructive probing of a Rydberg level opens up a wide range of possible experiments. In particular, we focus on two applications: First, we exploit the narrow linewidth of the EIT spectra to extend measurement of the nd series fine structure splitting up to $n = 96$. Second, we use Rydberg EIT to detect electric field transients in the gas phase produced by charge dynamics. The ability to continuously measure the local electric field could have useful applications in plasma physics or for detecting ions produced by either interactions between Rydberg atoms [6] or ionization of the Rydberg state by the excitation or trapping lasers [16].

The energy levels of ^{85}Rb relevant to this work and the experimental setup are shown in Fig. 1. The EIT ladder system consists of a weak probe beam resonant with a $5s^2S_{1/2}(F = 3) \rightarrow 5p^2P_{3/2}(F')$ transition and an intense coupling beam resonant with $5p^2P_{3/2}(F') \rightarrow nd^2D_{3/2}$ or $5p^2P_{3/2}(F') \rightarrow nd^2D_{5/2}$ as indicated in Fig. 1(a). The d state hyperfine splitting is negligible. The probe beam with wavelength $\lambda_p = 780.24$ nm, power 1 μW, and beam waist 0.4 mm ($1/e^2$ radius) propagates through a room temperature rubidium vapor cell of length 75 mm [Fig. 1(b)]. The transmission through the cell as the probe beam is scanned is monitored on a photodiode. The probe laser polarization is varied between linear (vertical or horizontal) and circular using appropriate wave plates. The

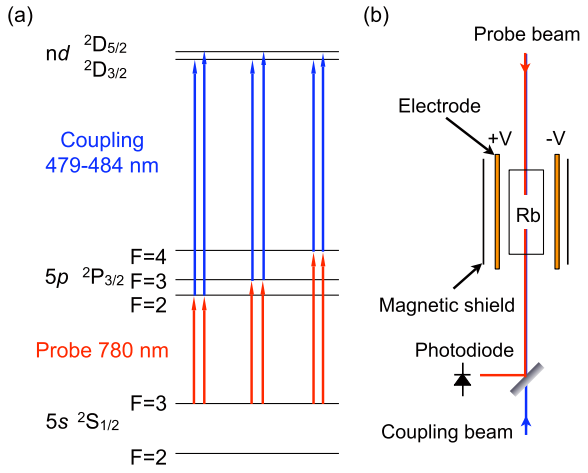

FIG. 1 (color online). (a) Energy level diagram of the ^{85}Rb ladder system. A probe beam at 780 nm measures the absorption on the $5s^2S_{1/2} \rightarrow 5p^2P_{3/2}$ transition, while an intense coupling beam at 480 nm dresses the $5p^2P_{3/2} \rightarrow nd^2D_{3/2,5/2}$ transition with $n = 26$–124. The fine and hyperfine splitting of the nd and $5p^2P_{3/2}$ states, respectively, give rise to six two-photon resonance lines. (b) A schematic of the experimental setup. The 480 and 780 nm beams counterpropagate through a room temperature Rb vapor cell. The transmission of the 780 nm light is detected on a photodiode. The vapor cell is placed between two electrodes inside a magnetic shield.

coupling beam with wavelength $\lambda_c = 479.2$–483.9 nm is produced by a commercial frequency doubled diode laser system (Toptica TA-SHG). The wavelength of the coupling laser is tuned using a commercial wave meter to the desired transition wavelength taken from Ref. [17]. The coupling beam counterpropagates through the cell with a power up to 200 mW, a waist of 0.8 mm ($1/e^2$ radius), and linear polarization in the vertical direction. The vapor cell is placed inside a μ-metal shield to reduce the effect of stray magnetic fields.

A typical spectrum corresponding to the ^{85}Rb $5s^2S_{1/2}(F=3) \rightarrow 5p^1P_{3/2} \rightarrow 44d$ ladder system is shown in Fig. 2. In Fig. 2(a), we show the probe absorption with the coupling laser tuned close to and far away from the $5p^2P_{3/2}(F=4) \rightarrow 44d^2D_{5/2}$ resonance. The frequency axis is calibrated using the known splittings between the $5p^2P_{3/2}$ hyperfine states [18]. Note that, due to the Doppler mismatch between the probe and coupling lasers, the hyperfine splitting of the $5p^2P_{3/2}$ state is scaled by a factor of $1 - \lambda_c/\lambda_p$ and the fine structure splitting of the nd state by λ_c/λ_p.

In Fig. 2(b), we show the difference between the resonant and far-detuned traces. The spectrum contains six lines corresponding to transitions between the $F = 2$, 3, and 4 hyperfine states in the $5p^2P_{3/2}$ state and both of the fine structure components $^2D_{3/2}$ and $^2D_{5/2}$ of the $44d$ state as indicated in Fig. 1(a). The position of the EIT peak within the Doppler broadened absorption profile is determined by the coupling laser detuning. For a coupling power of 180 mW, the largest peak corresponding to the $5p^2P_{3/2}(F=4) \rightarrow 44d^2D_{5/2}$ resonance produces a change in the probe transmission of 5%. This peak height is reduced and the width is increased by about a factor of 2 if we remove the magnetic shield. The observed spectra are not strongly dependent on the probe laser polarization. The linewidth of the EIT resonance is typically 2 MHz, which is significantly narrower than the natural width of the intermediate $5p$ states (6 MHz). Also apparent in Fig. 2(b) is that the line shape of the EIT feature displays enhanced absorption just below and above the two-photon resonance. This effect arises due to the wavelength mismatch between the coupling and probe lasers. Although the effect is known [19], it has not been observed in previous experiments. One can obtain a theoretical prediction for the EIT line shape using an approximate expression for the susceptibility derived in the limit of a weak probe [14]

$$\chi(v)dv = -i\frac{3\lambda_p^2}{4\pi}\gamma_2 N(v)dv\Big[\gamma_2 - i(\Delta_p - \boldsymbol{k}_p\cdot\boldsymbol{v}) + \frac{(\Omega_c/2)^2}{\gamma_3 - i[\Delta_p + \Delta_c - (\boldsymbol{k}_p + \boldsymbol{k}_c)\cdot\boldsymbol{v}]}\Big]^{-1}, \quad (1)$$

where $\Omega_{p,c}$, $\Delta_{p,c}$, and $k_{p,c} = 2\pi/\lambda_{p,c}$ are the probe or coupling laser Rabi frequencies, detunings, and wave vectors, respectively, and $N(v)$ is the number density of ^{85}Rb atoms with velocity v. The decay rates $\gamma_{2,3}$ are the natural widths of the intermediate and upper states in the ladder system. Additional line broadening mechanisms such as laser linewidth can be included in γ_3. By summing the contributions from the different hyperfine lines in the $5p^2P_{3/2}$ state (with appropriate weightings) and integrating the imaginary part of (1) over the velocity distribution for a room temperature vapor, one obtains the absolute absorption coefficient and, hence, the transmission through the vapor cell as a function of the probe detuning. Multiple levels in the upper state of the ladder system can be included by adding extra coupling terms in Eq. (1) [20]. Figure 3 shows the prediction of Eq. (1) in comparison to

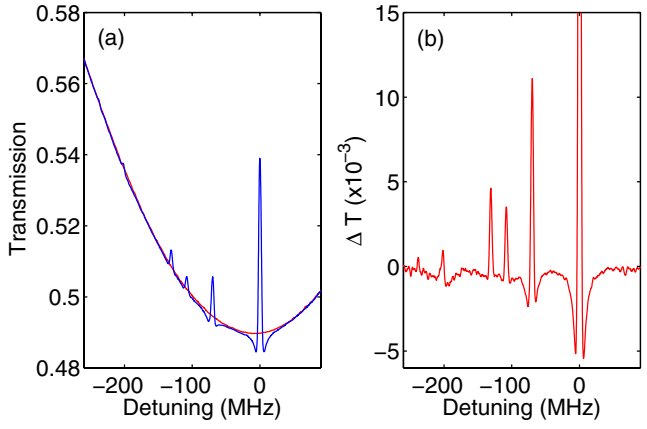

FIG. 2 (color online). (a) Probe transmission as a function of probe laser detuning near the ^{85}Rb $5s^2S_{1/2}(F=3) \rightarrow 5p^2P_{3/2}$ resonance with the coupling laser detuned nearly on resonance (red line) and far above resonance (blue line) with the $5p^2P_{3/2}(F=4) \rightarrow 44d^2D_{5/2}$ transition. (b) The change in the transmission ΔT is due to the coupling beam given by the difference between the two curves in (a). Six EIT resonances are observed.

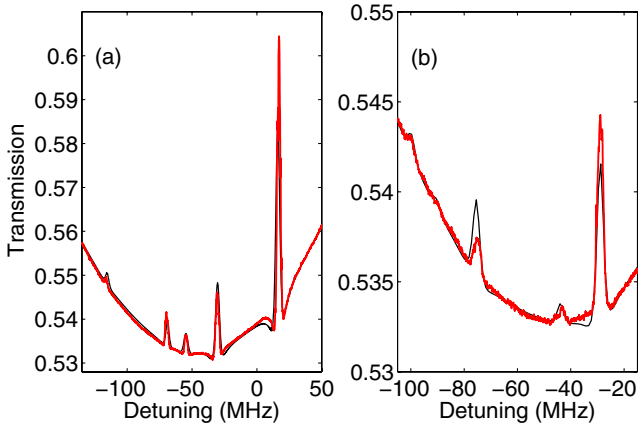

FIG. 3 (color online). Probe transmission as a function of detuning (thick red line) compared to Eq. (1) (thin black line) for (a) the $44d$ state with $\Omega_c = 2\pi(3.5$ MHz) and $\gamma_3 = 2\pi(0.3$ MHz) and (b) $80d$ with $\Omega_c = 2\pi(1.5$ MHz) and $\gamma_3 = 2\pi(0.3$ MHz).

the experimental data for (a) $n = 44$ and (b) $n = 80$. The only fit parameters are the Rabi frequency and detuning of the coupling laser, the rate γ_3, and the fine structure splitting of the d state. The enhanced absorption observed at higher Ω_c [Fig. 3(a)] is accurately predicted by Eq. (1).

For the $80d$ state [Fig. 3(b)], the change in the probe transmission is reduced to about 1%. This is consistent with the expected $1/n^{3/2}$ scaling of the coupling beam Rabi frequency. We can still observe the EIT resonance up to the $101d$ state and using lock-in detection up to $124d$. The EIT spectra give a direct measurement of the d state fine structure splittings. Previously, the fine structure splitting has been measured up to $n = 65$ using two-photon absorption and a thermionic diode to detect the ionized Rydberg atoms [21]. The fine structure splitting has also been observed by laser excitation and ionization of ultracold atoms [22–24]. We have measured the fine structure splitting of the nd series from $n = 39$ up to $n = 96$. In Fig. 4, we plot the measured splittings as a function of n together with a theoretical prediction using the quantum defect values from Ref. [25]. The measured splittings and the quantum defect prediction are in excellent agreement.

Next we investigated the effect of an external electric field on the Rydberg energy levels by applying a voltage between the electrodes shown in Fig. 1(b). We observe no effect on the EIT spectra for dc electric fields up to 100 V cm^{-1} regardless of the probe and coupling laser polarizations, suggesting that the Rydberg atoms are being screened. The main source of charge within the cell appears to be ions and electrons produced by photodesorption induced by the coupling laser at the surface of the cell [26]. For example, by retroreflecting the 480 nm laser with a glancing angle off the cell wall, we can create an asymmetry in the charge distribution that produces a 2.5 MHz splitting of the $70d$ line.

To further investigate the screening effect and charge dynamics within the cell, we studied the effect switching the electric field direction in a time of order 1 μs. For a dc field, the charges drift with a distribution which exactly compensates the applied field. However, if the field is switched in a time less than the charge relaxation time, there is incomplete cancellation of the applied field leading to a perturbation of the EIT signal. The relaxation time of the charge distribution is set by the transit time of a positive ion across the cell, which is of order 20 μs for a field of order 1 V/cm. To monitor the response of the EIT peak to a time varying field, we lock the probe laser to the $5s^2S_{1/2}(F = 3) \rightarrow 5p^2P_{3/2}(F = 4)$ transition using polarization spectroscopy [27] and tune the coupling laser to resonance with the $5p^2P_{3/2}(F = 4) \rightarrow 45d^2D_{5/2}$ transition. The change in transmission (ΔT) as the field is switched is shown in Fig. 5 (inset). Each time the field direction changes, the EIT peak is suppressed due to the transient penetration of the applied field. The duration of this transient depends linearly on the amplitude of the field and decreases exponentially with the coupling laser power; see Fig. 5. At higher power, the charge density is increased, and the distribution can relax faster towards the steady-state fully screened distribution. There is a small asymmetry between the response to increasing and decreasing field that depends on the alignment of the EIT probe relative to the center axis of the cell.

If we apply an rf frequency to the electrodes, then the time variation of the field is too fast for either the ions or the electrons to screen the field. In this case, the $^2D_{5/2}$ and $^2D_{3/2}$ resonances are split into 3 and 2 lines corresponding to their respective $|m_J|$ components, as shown in Fig. 6. Similar spectra have recently been observed by ionizing

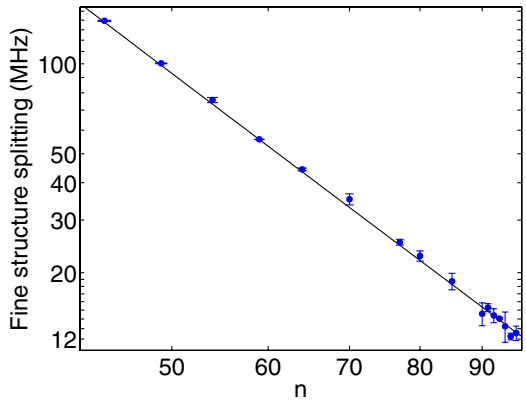

FIG. 4 (color online). The measured fine structure splitting (solid circles) of the d state as a function of the principal quantum number n. The line is calculated using the quantum defects from Ref. [25].

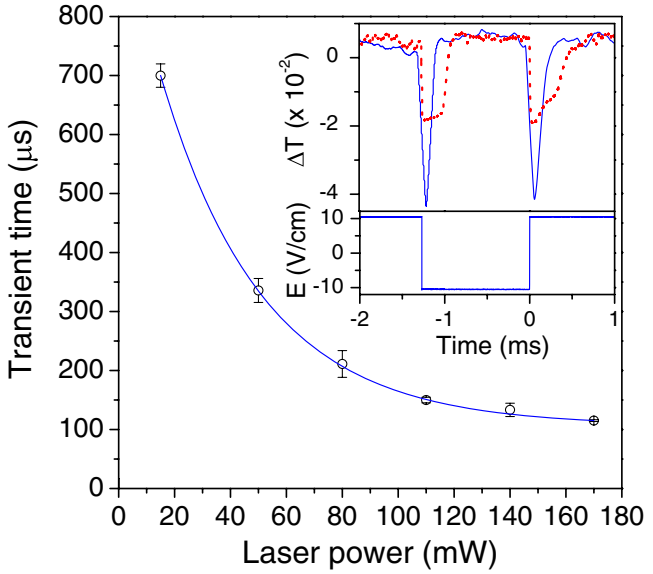

FIG. 5 (color online). The width (FWHM) of the EIT transient (rising edge) as the electric field is switched between ± 10 V/cm as a function of the coupling laser power. The transient time decays exponentially to a fixed value at high power. Inset: The transient EIT response for a coupling laser power of 50 (dashed line) and 170 mW. Note that the EIT peak height is smaller at lower coupling laser power.

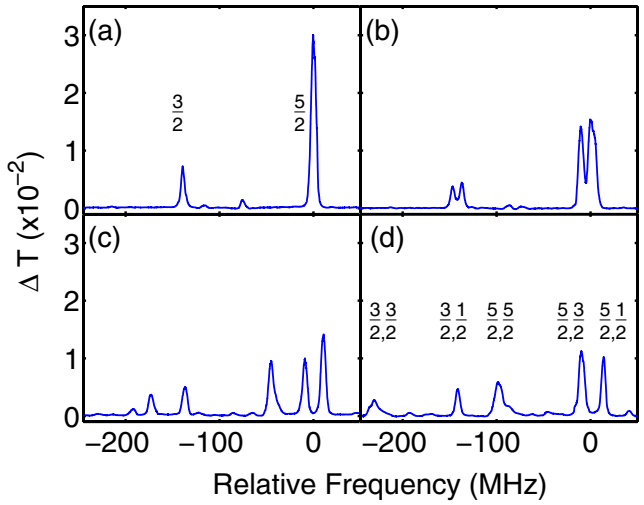

FIG. 6 (color online). EIT spectra observed by scanning the coupling laser across the $5p^2P_{3/2}(F=4) \rightarrow 44d^2D$ resonance with the probe laser locked to the $5s^2S_{1/2}(F=3) \rightarrow 5p^2P_{3/2}(F=4)$ transition. A higher probe power is used, so the lines are power broadened and the enhanced absorption effect is lost. An rf field with frequency 90 MHz and amplitude (a) 0.0, (b) 0.18, (c) 0.32, and (d) 0.48 V/cm is applied. The $^3D_{3/2}$ and $^2D_{5/2}$ lines, at -139 and 0 MHz in (a), are split into 2 and 3 $|m_J|$ components, labeled as J, $|m_J|$ in (d).

ultracold Rydberg atoms [24]. In a time varying field, one may not expect to observe narrow lines; however, due to the quadratic dependence on the electric field, the time dependence of the resonance lines has a rectified sin dependence, which has a large dc field component. The distortion of the line shape due to the time dependence of the field is most apparent in the $^2D_{3/2}(|m_J| = 3/2)$ and $^2D_{5/2}(|m_J| = 5/2)$ lines in Fig. 6(d), as they have the highest field sensitivity. These results indicate that, on a time scale faster than the charge relaxation time, the Rydberg states can be polarized even in the presence of a charged mean field. Consequently, dipole blockage effects could be observable in a thermal vapor, even though charge screening effects may be present.

In summary, we have demonstrated coherent optical detection of highly excited Rydberg states (up to $n = 124$) using EIT, providing a direct nondestructive probe of Rydberg energy levels. The observed spectra, displaying enhanced absorption below and above the Rydberg resonance, can be accurately predicted by the optical Bloch equations. The narrow linewidth of the EIT resonance allows us to extend measurements of the fine structure splitting of the nd series up to $n = 96$. We also show that the EIT spectra are sensitive to charge dynamics within the cell, offering the potential for direct optical detection of electric field fluctuations in the gas phase. In our experiment, the density of atoms participating in the EIT resonance [28] is more than 2 orders of magnitude lower than the density used in the observation of dipole blockade [5]. In future work, we will apply the technique to higher density vapors to investigate dipole blockade effects and their potential application in photon entanglement [9].

We are grateful to S. L. Cornish, I. G. Hughes, M. P. A. Jones, and R. M. Potvliege for stimulating discussions and A. P. Monkman for the loan of equipment. We also thank the EPSRC for financial support.

[1] T. F. Gallagher, *Rydberg Atoms* (Cambridge University Press, Cambridge, England, 1994).
[2] I. Mourachko *et al.*, Phys. Rev. Lett. **80**, 253 (1998).
[3] M. P. Robinson *et al.*, Phys. Rev. Lett. **85**, 4466 (2000).
[4] T. C. Killian *et al.*, Phys. Rev. Lett. **86**, 3759 (2001).
[5] T. Vogt *et al.*, Phys. Rev. Lett. **97**, 083003 (2006).
[6] W. Li, P. J. Tanner, and T. F. Gallagher, Phys. Rev. Lett. **94**, 173001 (2005).
[7] D. Jaksch *et al.*, Phys. Rev. Lett. **85**, 2208 (2000).
[8] M. D. Lukin *et al.*, Phys. Rev. Lett. **87**, 037901 (2001).
[9] I. Friedler, D. Petrosyan, M. Fleischhauer, and G. Kurizki, Phys. Rev. A **72**, 043803 (2005).
[10] T. Cubel *et al.*, Phys. Rev. A **72**, 023405 (2005).
[11] J. Deiglmayr *et al.*, Opt. Commun. **264**, 293 (2006).
[12] K.-J. Boller, A. Imamolu, and S. E. Harris, Phys. Rev. Lett. **66**, 2593 (1991); A. Kasapi, M. Jain, G. Y. Yin, and S. E. Harris, Phys. Rev. Lett. **74**, 2447 (1995).
[13] M. Fleischhauer, A. Imamoglu, and J. P. Marangos, Rev. Mod. Phys. **77**, 633 (2005).
[14] M. Xiao, Y. Q. Li, S. Z. Jin, and J. Gea-Banacloche, Phys. Rev. Lett. **74**, 666 (1995).
[15] J. Clarke, H. Chen, and W. A. van Wijngaarden, Appl. Opt. **40**, 2047 (2001).
[16] R. M. Potvliege and C. S. Adams, New J. Phys. **8**, 163 (2006).
[17] B. P. Stoicheff and E. Weinberger, Can. J. Phys. **57**, 2143 (1979).
[18] U. D. Rapol, A. Krishna, and V. Natarajan, Eur. Phys. J. D **23**, 185 (2003).
[19] A. Krishna, K. Pandey, A. Wasan, and V. Natarajan, Europhys. Lett. **72**, 221 (2005).
[20] S. D. Badger, I. G. Hughes, and C. S. Adams, J. Phys. B **34**, L749 (2001).
[21] K. C. Harvey and B. P. Stoicheff, Phys. Rev. Lett. **38**, 537 (1977).
[22] B. K. Teo *et al.*, Phys. Rev. A **68**, 053407 (2003).
[23] K. Singer *et al.*, Phys. Rev. Lett. **93**, 163001 (2004).
[24] A. Grabowski *et al.*, Fortschr. Phys. **54**, 765 (2006).
[25] W. Li, I. Mourachko, M. W. Noel, and T. F. Gallagher, Phys. Rev. A **67**, 052502 (2003).
[26] J. H. Xu *et al.*, Phys. Rev. A **54**, 3146 (1996).
[27] C. P. Pearman *et al.*, J. Phys. B **35**, 5141 (2002).
[28] The density of ^{85}Rb at room temperature is 2×10^{10} cm^{-3}; however, due to Doppler broadening, less than 1% of the atoms are resonant with the two-photon EIT transition. By solving the optical Bloch equations for the parameters of the experiment, one finds that the maximum Rydberg atom density is much less than 10^8 cm^{-3}.